Cellulose (2015) 22:2529–2541
DOI 10.1007/s10570-015-0650-y

ORIGINAL PAPER

Physical and chemical reinforcement of chitosan film using nanocrystalline cellulose and tannic acid

Viyapuri Rubentheren · Thomas A. Ward · Ching Yern Chee · Praveena Nair

Received: 8 January 2015 / Accepted: 3 May 2015 / Published online: 9 May 2015

Abstract Chitosan film with nanocrystalline cellulose (NCC) as a physical reinforcement and tannic acid as a chemical crosslinker was prepared by the casting evaporation method. The objective was to improve its mechanical properties, reduce its moisture content and solubility, and maintain its biodegradability. This was done to examine its potential suitability as an ultra-lightweight wing membrane for a future biomimetic micro air vehicle. Different contents of nanofiller material and tannic acid were added to a chitosan matrix and comparisons were made with neat chitosan film. Mechanical test shows that the addition of NCC into the chitosan matrix improves the tensile strength by 69.8 % compared to neat chitosan. Insertion of tannic acid to the nanocomposite film further improves the tensile strength by 82.6 %. These reinforcement materials also reduce the moisture content up to 73.5 % and water solubility to 67.9 %. Morphological studies were carried out using transmission electron microscopy (TEM), scanning electron microscopy (SEM) and an ultraviolet–visible spectrophotometer. The TEM images revealed the presence of nano-sized cellulose particles with high aspect ratios (average of 20.9). SEM images were examined to reveal the dispersion level of NCC and the effects of tannic acid in the film. Fourier-transform-infrared spectroscopy imagery was used to define the interaction of the molecules. X-ray diffraction analysis confirms that the addition of NCC increases the presence of crystalline structures in the film, which makes it more rigid. The addition of tannic acid changed the structure into an anhydrous crystalline conformation, when compared to neat chitosan film.

Keywords Chitosan film · Crosslinking · Nanocrystalline cellulose · Tannic acid · Nanocomposite

V. Rubentheren · T. A. Ward (✉) · C. Y. Chee · P. Nair
Department of Mechanical Engineering, University of Malaya, 50603 Kuala Lumpur, Malaysia
e-mail: DrTomWard@hotmail.com; DrTomWard@um.edu.my

Introduction

Throughout the ages, nature has inspired many biomimetic innovations that have advanced the technological achievements of civilizations (Parker 2010). Polysaccharides are of interest for emerging engineering applications because they are lightweight, biodegradable, and widely distributed in nature. These biopolymers have many potential applications, ranging from structural applications to packaging materials. The benefits of these materials are becoming increasingly realized as the properties are studied and better understood (Syed et al. 1999; Takegawa et al. 2010). The use of lightweight structural materials are important in many applications (e.g. aircraft, ground vehicles, packaging, biomedical applications, etc.) in

order to improve its cost and performance (Goede et al. 2009). Recent studies on biomimetic air vehicles (BMAV) have motivated researchers to look for high performance lightweight materials. BMAV are a type of micro-scaled flapping winged aircraft that mimics the flapping wing motion of insects, birds or bats (Orlowski and Girard 2012). BMAV are envisioned for use in engineering maintenance, safety inspections, and police or military surveillance operations. Their lightweight, micro-sized structure allows them to easily fly into confined spaces or hazardous environments with micro-scaled cameras or sensors. Researchers are now studying swarm technology with the objective of distributing a group of BMAV in prescribed flying patterns (Kushleyev et al. 2013). In order for this to be implemented in a cost effective manner, the BMAV must be mass produced using inexpensive materials. Also due to power and range limitations, missions may be performed one-way, with no intention to return the BMAV to its original launch point. These requirements predicate the need for BMAV to be fabricated from bio-degradable materials (similar to insects). The wing membrane is generally the largest part of BMAV designs. So there is much interest in fabricating lightweight biodegradable films for use as wing membranes.

A dragonfly's wing membrane is mostly composed of chitin. Although chitin is abundantly available in nature, it is underutilized in commercial applications because of its intractable bulk structure and insolubility to common organic solvents. In order to solve these problems, chitosan was examined. Chitosan is a biodegradable and biocompatible natural polysaccharide composed of linear polysaccharide 1,4 -linked 2-amino-deoxy-β-D-glucan (Badawy and Rabea 2014). Chitosan is the *N*-deacetylated derivative of chitin. It has an excellent film forming capability, giving it a great potential as a membrane for BMAV. However, chitosan film itself has poor mechanical and barrier properties that make it unsuitable for BMAV membrane applications as well as other applications (packaging). For these reasons, biopolymers are often blended with reinforcement material to enhance its properties. Complex fillers such as carbon nano-tubes and graphene oxide have been successfully incorporated into a chitosan matrix to enhance its barrier and mechanical properties (Kroustalli et al. 2013; Zuo et al. 2013). Since these fillers are expensive and complex, alternative materials such as cellulose is examined in this article.

Cellulose has excellent reinforcement, renewable and biodegradable properties. Naturally occurring microfibrils from cellulose molecules in plants and some marine creatures often act as a reinforcing structure (Moon et al. 2011). Cellulose consist of long chain polysaccharide composed of β-1,4 linked D-glucose rings (Cranston and Gray 2006). Nano sized single crystal cellulose (commonly referred as nanocrystalline cellulose, nanowhiskers or nanofibrils) can be extracted from various cellulose sources by the acid hydrolysis process (de Souza Lima and Borsali 2004). Nanocrystalline cellulose (NCC) is highly crystalline nanometer sized rod-like particle prepared as an aqueous colloidal suspension. The use of NCC as a reinforcement material has been proven to increase the mechanical and barrier properties by forming a percolation network and hydrogen bonding between the filler material and the polymers (Leung et al. 2013; Miao and Hamad 2013; Kabiri and Namazi 2014).

Besides adding filler material, biopolymers can be chemically modified to enhance its properties by using crosslinking agents that change the structure of the matrix (Bigi et al. 2001; Sabato et al. 2001). Although many crosslinking agents are available, glutaraldehyde is most often used, because it has a proven ability to enhance mechanical and water resistivity (Bigi et al. 2001). But, since glutaraldehyde is synthetic and cytotoxic, it is not suitable for applications that require biocompatibility. Tannic acid on the other hand is not cytotoxic. It has been used as a crosslinker in gelatin films with good performance results (Cao et al. 2007). Tannic acid, also known as hydrolysable tannins, obtained from the galls of Rhus chinensis (Chinese sumac or nutgall tree). It has a multiple phenolic groups with high molecular weights having an antioxidant capability (Henson et al. 2004).

The objective of this research is to process chitosan film and study the effects of NCC used for physical reinforcement and tannic acid as a crosslinking agent for chemical reinforcement. We have found no research publications that investigate the effect of using these two reinforcing materials in a chitosan matrix. Its mechanical properties and water uptake will then be compared to previous results that used chitin whiskers as a filler material (Rubentheren et al. 2015).

Experimental methodology

Materials

Chitosan powder (with minimum deacetylation degree of 75 %) and microcrystalline cellulose (MCC) were purchased form Sigma-Aldrich (Malaysia). Glacial Acetic acid grade AR and tannic acid were purchased from Friendemann Schmidt. Sulfuric acid and other agents were provided by Fisher Scientific and used as received.

Methods

The NCC was prepared using the acid hydrolysis method described by Bondeson et al. (2006), with a slight modification. The first step begins by mixing 10.2 g of MCC with distilled water in a beaker. The mixture was then put in an ice bath and stirred while concentrated sulfuric acid was carefully added by drops (to avoid a temperature spike) until the desired acid concentration of 63.5 wt% was reached. The suspension was heated in a flat bottom flask under constant stirring (using a Corning PC-420D magnetic stirrer) for 130 min at 45 °C. After acid hydrolysis, the suspension was centrifuged at 6000 rpm for 10 min, followed by removal of the sulfuric acid solution from the container. Distilled water was added into the container to dilute it and then re-centrifuged. This step was repeated three times. Next, the NCC slurry was collected and transferred into a dialysis bag. The slurry was dialyzed in running water for 24 h; and then soaked in distilled water for another 24 h to stabilize the pH to a neutral state. Once neutralized, the dispersion was completed by 10 min of ultrasonic treatment. Five drops of chloroform was then added to prevent bacterial growth. Finally, the suspension was refrigerated in an air tight container at 6 °C with a final concentration of 4.6 wt% of NCC.

Chitosan solution was prepared by adding 2 wt% of chitosan powder into a 2 % (v/v) acetic acid solution under vigorous magnetic stirring for 1 h at 90 °C. The mixture was then cooled to room temperature. NCC was slowly added into the solution. To obtain a homogenized suspension, the mixture was treated with a high speed homogenizer for 5 min, then with 20 min of magnetic stirring. The mass ratio of NCC to chitosan was controlled at 0:100, 10:90, 30:70, and 50:50. The mixed suspension was cast onto a plastic Petri dish. The cast suspensions were left overnight in a dry cabinet to remove bubbles and later evaporated in a drying oven at 40 °C for 48 h to obtain dry composite films. The theoretical dry weight of the film was 0.5295 g with an average thickness of 0.09 mm.

For the crosslinking process, different amounts of tannic acid were used before the NCC was added. A batch of 20 or 40 mg of tannic acid per 1 g of chitosan was added into the suspension under vigorous magnetic stirring for another 1 h at 90 °C, until it was homogenized. Table 1 shows twelve different types of composite films (Set I: neat chitosan film, serving as the control sample; Set II: crosslinked chitosan film; Set III: chitosan film embedded with NCC; Set IV: crosslinked chitosan film embedded with NCC).

Material characterization

Table 2 lists the characterization equipment used in this analysis. All samples were stored in dry cabinet prior to testing. For film solubility and water uptake studies, 15 × 12 mm samples were prepared. Samples were heated in a convention oven at 105 °C for 1.5 h and weighed to the nearest 0.0001 g (dry weight). Water uptake was measured by immersing the dried film pieces in 75 ml of distilled water for 1 h at 25 °C. Then samples were removed and dried with filter paper to absorb excess surface water and weighed again (wet weight). The percentage of water uptake was calculated using Eq. (1):

$$\%\,\text{water uptake} = \left[\frac{(W_s - W_i}{W_i}\right] \times 100 \qquad (1)$$

where W_s is the weight of the swollen sample and W_i is the weight of the sample after heating it in a convection oven. Solubility tests were performed immediately after recording the swollen weight as mentioned above. The samples were dried in a convection oven at 105 °C (for at least 1 h 30 min) until it reached a constant dry weight. The samples were weighed to the nearest 0.0001 g. This dry weight was then used in Eq. (2) to find the solubility:

$$\%\,\text{solubility} = \frac{\text{initial dry weight} - \text{final dry weight}}{\text{initial dry weight}} \times 100 \qquad (2)$$

Table 1 Nomenclature of the composite film sets studied

Sample set	Sample code	Chitosan (%)	NCC (%)	Tannic acid (mgTA/chitosan)
I	Control	100		
II	A	100		20
	B	100		40
III	A	90	10	
	B	70	30	
	C	50	50	
IV	A	90	10	20
	B	70	30	20
	C	50	50	20
	D	90	10	40
	E	70	30	40
	F	50	50	40

Table 2 Characterization equipment used in this research

Instrument	Model	Parameters
Transmission electron microscopy (TEM)	Zeiss EFTEM Libra 120	500 nm magnification for all samples
Scanning electron microscopy (SEM)	Zeiss Evo MA10	2.00 K (2 μm) magnification for all samples dipped in liquid nitrogen in order to fracture
UV–visible spectrophotometer	Cary 50 Probe	Light range between 200 and 800 nm
Fourier transform infrared spectroscopy (FTIR)	Perkin Elmer Spectrum 400 FT-IR/FT-FIR spectrometer	32 scans at 4 cm^{-1} resolution Measurements were recorded between 4000 and 400 cm^{-1}
X-ray diffraction (XRD)	Siemens D5000	Cu Kα radiation source (k = 1.540600 Å) Operating at 40 kV and 40 mA at room temperature Scattering range of (2θ) 5-80° with a step size of 0.1
Universal testing machine (UTM)	Shimadzu AGS-X series	100 N load cell Crosshead speed of 1 mm/min Sample size of 50 mm by 8.5 mm with at least 5 samples for each test accordance to ASTM D882-02

Results and discussion

Microstructural studies by transmission electron microscope (TEM)

The NCC structure was studied using a transmission electron microscope (TEM). Figure 1 shows TEM images of NCC in suspension form. The individual nanocrystals were shaped as long slender rods, having an average aspect ratio of 20.9. The TEM image in Fig. 1a shows that the length of NCC in a range between 150 and 450 nm (with an average value being ~320 nm). Figure 1b shows the diameters of the NCC in a range between 15 and 40 nm (with an average value being ~29 nm). Similar results were obtained from Peng et al. (2011) where the average value of NCC derived from microcrystalline cellulose was 500 nm in length and 10 nm in width. These nano sized materials exhibit colloidal behavior, due to negative charge repulsion among the nanocrystalline particles. This promotes good dispersion of the suspension, as described by (Zhong et al. 2012).

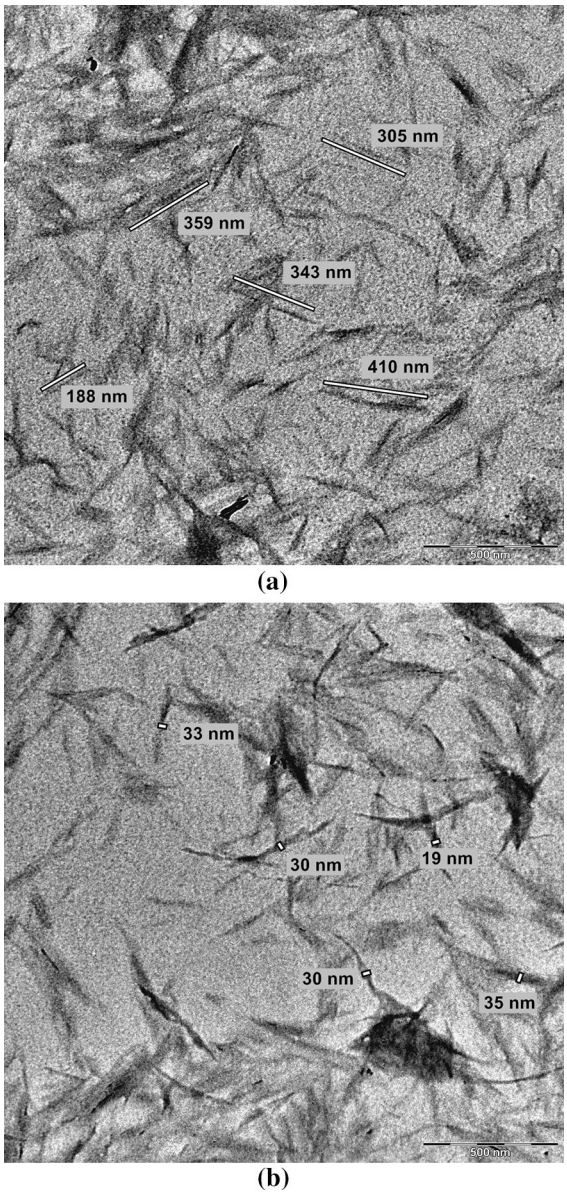

Fig. 1 TEM images of NCC in aqueous medium, **a** magnified at 500 nm with measured length, **b** magnified at 500 nm with measured width

Morphological characterization by scanning electron microscope

A scanning electron microscope (SEM) was used to inspect the film. SEM reveals the dispersion level of the NCC within the chitosan matrix and the effects of tannic acid. Figure 2a–d shows a SEM micrograph of the film surface. Figure 2e–h shows a SEM micrograph of the fractured cross-section of the chosen films: Set I, Set II (B), Set III (C) and Set IV (F). (The sample was fractured after it was cooled with liquid nitrogen.) The control film in Fig. 2a appears to be a smooth and homogeneous surface, which indicates good miscibility in the aqueous media. The cross-linked film (shown in Fig. 2b) leads to the formation of a more porous surface. Addition of NCC (in Fig. 2c) results in the film forming more ridges and an uneven surface. Dense white rod structures also appear in the Set III (C) film, which correspond to cellulose nanocrystals as reported by Azizi Samir et al. (2005). However, the SEM image of the Set IV (F) film (in Fig. 2d) shows less roughness and a more homogenized structure, when compared to film Set III (C). This is due to the role played by tannic acid, which interacts with the NCC and chitosan matrix, as seen in FITR spectra. Figure 2e, f of Set I and Set II (B) does not show much difference, except for surface roughness and the appearance of cracks in both cross sections. However, both Fig. 2g, h show increased surface roughness and fiber-like formations. This indicates aggregation of NCC and phase separation occurrence for the Set III (C) and Set IV (F) films, as reported by Zhao et al. (2014). It is clear that the addition of NCC caused drastic changes in the film's microstructure. The addition of tannic acid makes the film more porous. SEM analysis further clarifies the enhanced mechanical and water resistivity properties, due to the introduction of NCC and tannic acid.

Optical transmittance

The visible light transparency for all sample sets is shown in Fig. 3. The printed letter "Sample" can be seen for all sample sets. Generally all sample sets exhibit a slight yellow appearance. The addition of tannic acid tends to make the film appear more yellowish due to oxidative reactions, as discussed by Rivero et al. (2010). The word "Sample" becomes more blurred with increasing NNC loading. The optical transmittance (Tr) data (for a wavelength interval of 200–800 nm) for selected sample sets is shown in Fig. 4. Film Set I exhibits the highest optical transparency. The addition of tannic acid for Set II reduces the transparency, especially in the range below 700 nm. The transparency significantly decreases as the loading of NCC increases [Set III (C)]. There is a significant difference in transparency between 350 and 450 nm for the sample sets

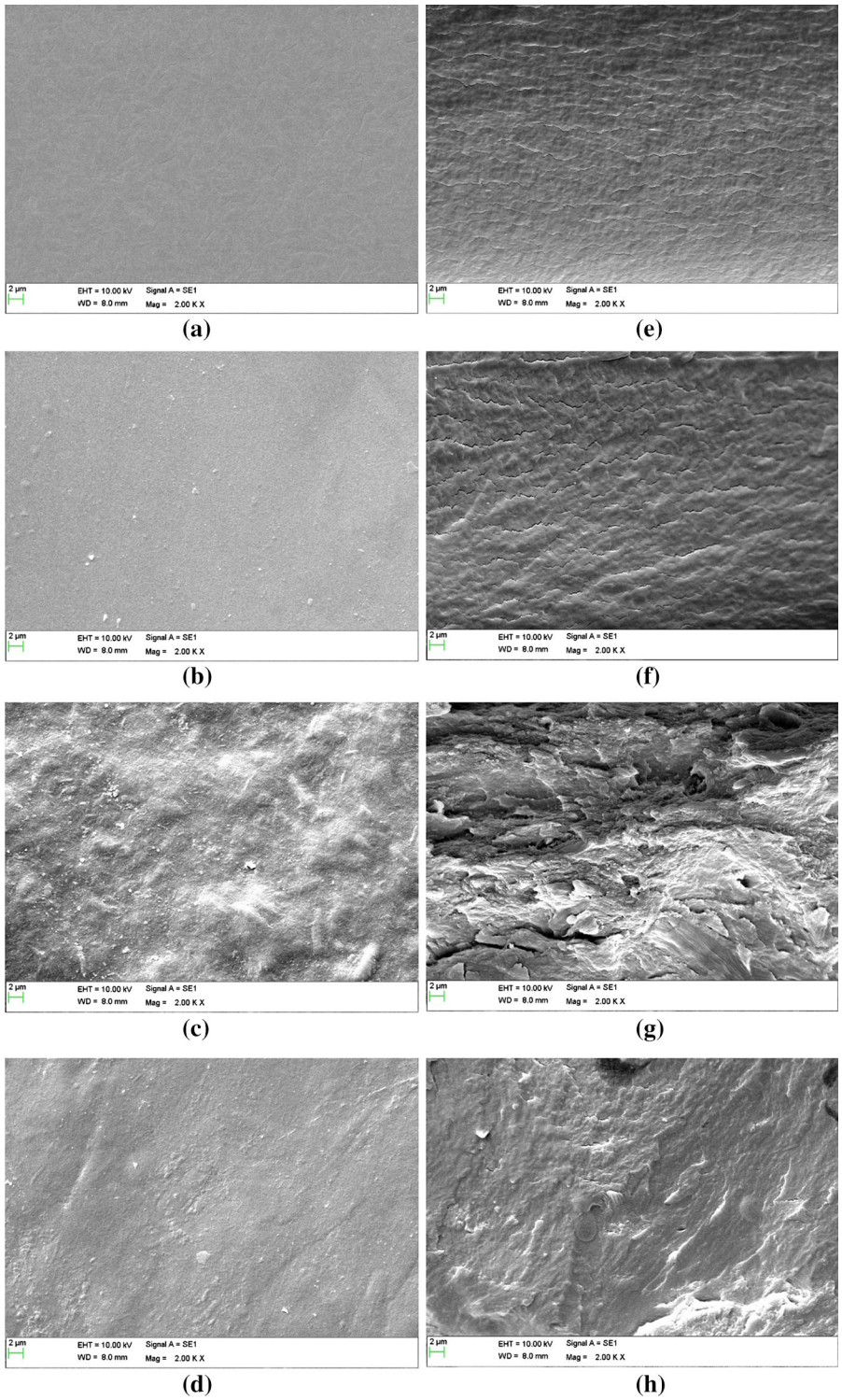

Fig. 2 SEM micrograph of surface, **a** Set I; **b** Set II (B); **c** Set III (C); and **d** Set IV (F); cross-section, **e** Set I; **f** Set II (B); **g** Set III (C); and **h** Set IV (F)

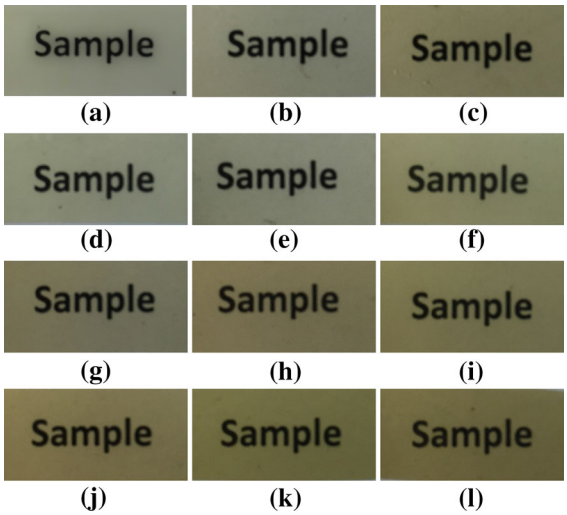

Fig. 3 Appearance of all sample sets: **a** Set I; **b** Set II (A); **c** Set II (B); **d** Set III (A); **e** Set III (B); **f** Set III (C); **g** Set IV (A); **h** Set IV (B); **i** Set IV (C); **j** Set IV (D); **k** Set IV (E); **l** Set IV (F)

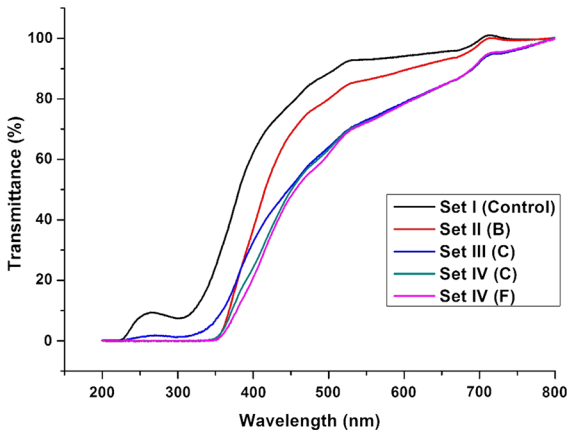

Fig. 4 UV–visible spectrophotometer of chosen sample sets

having both NCC and tannic acid [Set III(C) and IV(F)]. This is due to aggregation of NCC particles in the chitosan matrix and the influence of oxidative process accelerated by tannic acid, which scatters the light much more for these films than the control set (Set I) and Set II.

Fourier-transform-infrared spectroscopy (FTIR)

A Fourier transform infrared (FTIR) spectroscopy was used to characterize the effect of NCC as a reinforcement filler and tannic acid as a crosslinker to the chitosan film. Figure 5 shows FTIR spectra of all the sample sets. The neat chitosan film Set I (Fig. 5a)

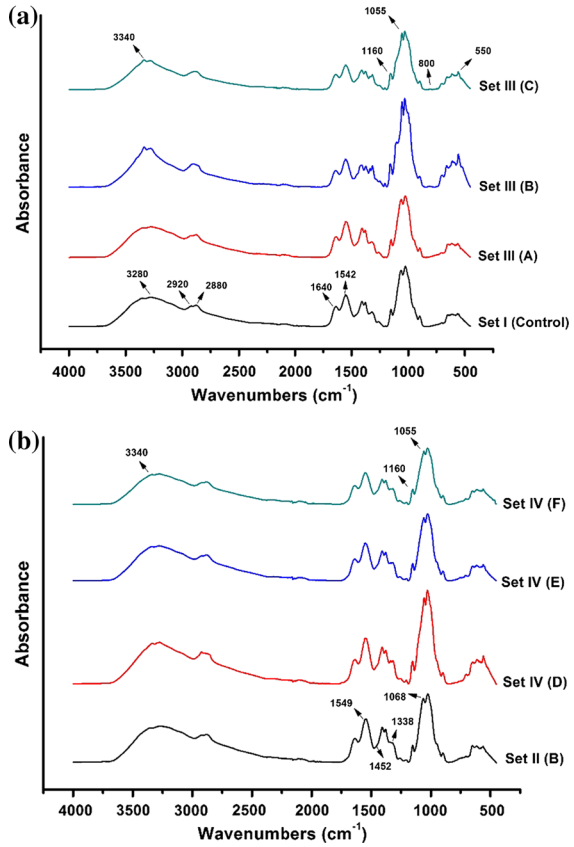

Fig. 5 FTIR spectra of: **a** non-crosslinked chitosan film, **b** crosslinked chitosan film (40 mg)

produced a wide spectrum across 3000–3600 cm^{-1} with a maximum absorption at ~3280 cm^{-1}. These results can be attributed to O–H and N–H stretching vibrations. Bands at 2880 and 2920 cm^{-1} are characteristic of methyl (CH3) anti-symmetric and symmetric stretching vibrations. These results agree with past published work (Ma et al. 2014). The visible absorption bands at 1640 cm^{-1} can be attributed to C=O stretching (amide I). The band at 1542 cm^{-1} is due to NH bending vibrations (amide II). Finally the absorption band at 1024 cm^{-1} is the vibration involving C–O group stretching of the chitosan film, as reported in (Leceta et al. 2013; Brugnerotto et al. 2001).

Film Set III (B and C) exhibited an increase in absorbance in a range between 3000 and 3600 cm^{-1}, with a sharp peak at 3340 cm^{-1} when compare to the neat chitosan (Set I). Past reporting identifies that these peaks are typical of O–H vibrations of NCC. The sharp peak indicates the occurrence of hydrogen

bonding between chitosan and NCC (Khan et al. 2012). The intensity of the bands at 1160 and 1055 cm^{-1} increased. These bands are related to cellulosic compounds, assigned to C–O, C–C and ring structures. The increased peaks of the bands between 800 and 650 cm^{-1} is due to O–H out of plane bending vibrations (Nikonenko et al. 2005). These observations indicate that there is good miscibility between the NCC and the chitosan matrix.

Film in Set II (B) (Fig. 5b), showed an increment in band peak located at 1549 cm^{-1}, which was not present in Set I. This is due to the symmetrical deformation of NH3+ group, resulting from the ionization of the primary amine group in the presence of carboxylic group. A weak band appeared at 1452 cm^{-1}, which indicates electrostatic interaction of carboxyl group. The band 1068 cm^{-1} (attributed to the C–O–C bonding vibration) was attenuated and band 1338 cm^{-1} disappeared when compared to the neat chitosan (Set I) film spectra. These changes indicate interactions between the chitosan amino group and the carboxyl group located in tannic acid, as reported by Aelenei et al. (2009). Film Set IV (F) (Fig. 5b) has visible peaks at 1160 and 1055 cm^{-1} that does not change, which is due to NCC loading in the crosslinked film. The band at 3340 cm^{-1} seems to be reduced for the cross-linked film. This indicates that the hydrogen bonding between NCC and chitosan is being disturbed by the tannic acid.

X-ray diffraction (XRD)

A structural analysis of all the sample sets was performed using the X-ray diffraction method. Figure 6 shows the X-ray diffractograms of four samples, one for each sample set. The four samples were selected because each has the highest concentration of additives within their particular set. These samples are: Set I (control), Set II (B) 100 % chitosan with 40 mg of tannic acid, Set III (C) 50 % of NCC, and Set IV (F) 50 % of NCC with 40 mg of tannic acid. Neat chitosan exhibited a sharp peak at $2\theta = 11.4°$ and a broader peak at $2\theta = 22.6°$. The sharp peaks are associated with hydrated "tendon" conformations and the broader peak indicates the existence of amorphous structures in the chitosan film (Wang et al. 2005). The two other minor peaks, located at 18.1° and 9.3°, also agree with past research (Ritthidej et al. 2002). Sample Set II (B) shows peaks in the region at $2\theta = 15°$, and

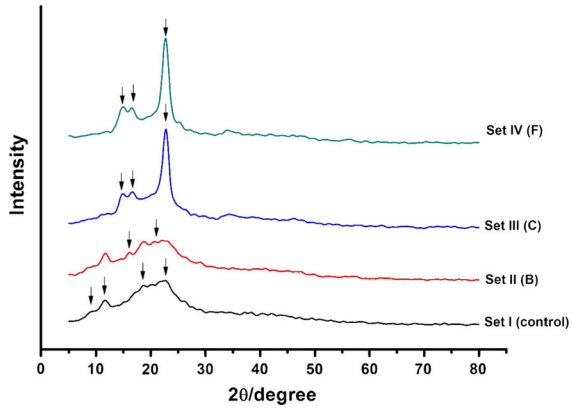

Fig. 6 Comparison of X-ray diffractograms of chosen sample sets

21°, which was not available for sample Set I. The addition of tannic acid raises the peak that exhibits the characteristic of anhydrous ("annealed") crystalline conformation (Rivero et al. 2011). In this present work, all films in Sets II and IV exhibited similar behaviors at $2\theta = 15°$.

Sample Sets III and IV have significantly elevated peaks compared to Set I, due to the introduction of NCC. Sets III (C) and Set IV (F) exhibit their highest scattering intensities at: $2\theta = 22.4°$, 16.5° and 14.5°, which correspond to the (1 1 0), (1 1 0), and (2 0 0) planes of the cellulose I crystal type, according to (Ma et al. 2011). This shows that NCC has a higher degree of crystallinity. The addition of NCC resulted in a strong scattering peak of cellulose signature, which becomes more significant with increasing filler content. Characteristics of the amorphous chitosan in the range of $2\theta = 20°–23°$, were super-positioned with the peaks of NCC. This shows that the films in Set III and IV exhibit a combination of amorphous and crystalline regions.

Mechanical properties

The measured mechanical properties of all the sample sets are shown in Fig. 7. The control film (Set I) exhibits the lowest tensile strength of 33.7 MPa, with the highest maximum elongation-at-break of 43.6 % (Fig. 7a, b). With the addition of NCC, the tensile strength increases significantly [Set III (B and C)] and the elongation-at-break is drastically reduced. Set III (C) records the highest tensile strength of 57.2 MPa for a non- crosslinked film, with an elongation-at-

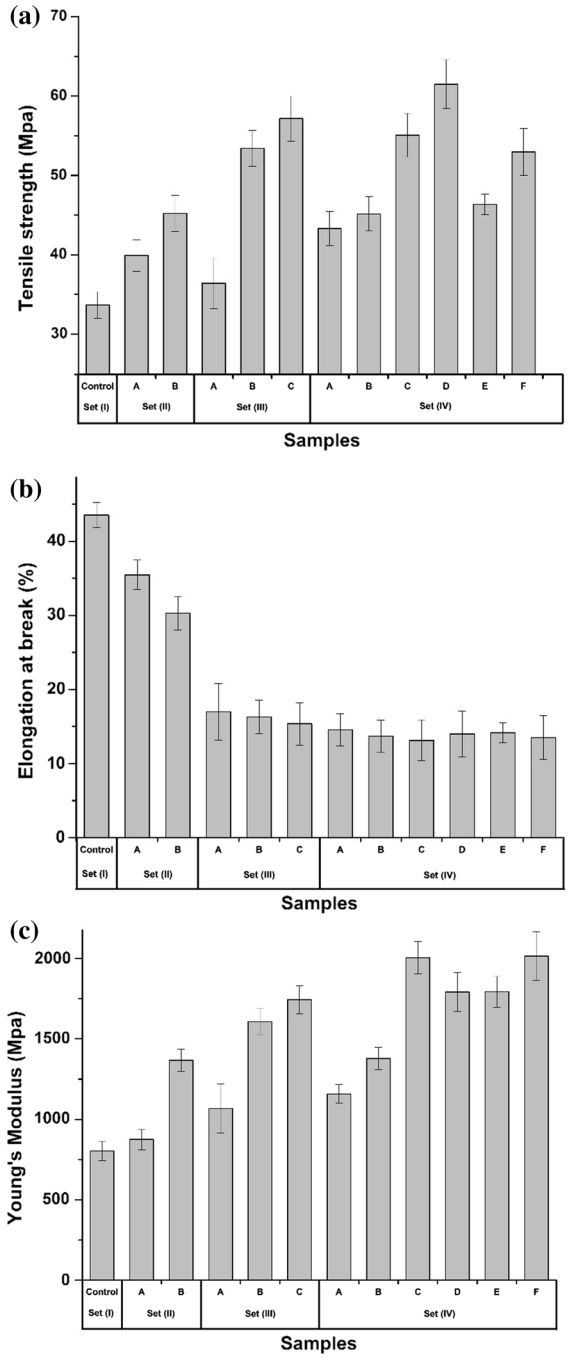

Fig. 7 Mechanical properties of all sample sets, **a** tensile strength, **b** elongation-at-break, **c** Young's modulus

break of 15.4 %. The tannic acid crosslinker also increases the tensile strength in sample Set II and IV. A steady increment was observed in sample Set II. Set II (B) recorded a tensile strength of 45.2 MPa with an elongation-at-break of 30.3 %. Set IV (D) had the highest tensile strength of 61.5 MPa. This is 82.6 % increase when compared to neat chitosan and has an elongation-at-break of 14.0 %. The addition of tannic acid appears to have no effect on the elongation of the Set IV nanocomposite films. The addition of NCC and tannic acid (Set II, III and IV) increases the Young's Modulus (stiffness) of the chitosan matrix (Fig. 7c). The Set IV films have much greater stiffness than Set I. In fact, films in Set III (C), Set IV (C, D, E and F) are more than twice as stiff as Set I.

These results show that the composite films have superior tensile strength and Young's modulus compared to neat chitosan film (Set I), due to the reinforcement effect of the crosslinker (Sets II and IV) and NCC (Sets III and IV). The increase in tensile strength caused by adding NCC in the chitosan film can be attributed to the reinforcing effect through effective stress transfer from the nanocrystals and chitosan polymer interface. Another researcher de Mesquita et al. (2010) postulated that the interaction between the anionic sulphate groups of NCC and the cationic amine groups of the chitosan promotes good bonding between them and this may lead to higher tensile strength. The TEM images and XRD diffractograms show that the NCC has a rod-like shape with a high aspect ratio and possesses a high degree of crystallinity. This is another contributory factor that increases its mechanical properties. However, the tensile increment difference between films in Set III (A, B) and (B, C) is large. This shows that increasing the nanocrystal content causes the tensile strength to exponentially increase until it reaches a threshold. There is a possibility that it will reach a maximum value and gradually decrease with additional filler loading. This is due to the aggregation of NCC. A similar trend was reported in past research by Li et al. (2009), where the optimum loading of cellulose nanocrystal was 15–20 % (w/w) before it reached the percolation threshold. The addition of NCC tends to make the film more rigid due to higher crystalline structure. This results in a reduction of the percentage of elongation-at-break. This behavior was also reported by Lu et al. (2004), who showed that the addition of chitin whiskers in soy protein isolate film reduces the percentage of elongation-at-break.

Crosslinking the chitosan film also increases the tensile strength and Young's modulus. This is due to the formation of a more stable network between the chitosan and tannic acid. A similar result was obtained

in past research, where the addition of tannic acid into chitosan film increased the tensile strength (Rivero et al. 2010). Introduction of tannic acid to the Set IV films only increases the tensile strength of the films in Set A and D. Other sample sets resulted in decreased tensile strength, but the Young's modulus increased. This can be attributed to two factors. Firstly the higher loading of tannic acid disturbs the NCC crystal network formation in the chitosan matrix. According to Gopalan Nair and Dufresne (2003) who studied chitin addition in natural rubber, the strength of the chitin network in the crosslinked natural rubber matrix is lower than unvulcanized rubber. They concluded that the chemical crosslinking of the matrix interferes with the formation of the chitin network, thus lowering the tensile strength. Secondly, as reported in morphological studies, a slight phase separation takes place in the nanocomposite material as tannic acid loading is increased. Peña et al. (2010) reported that this phase separation reduced the tensile strength, as more tannic acid was added into the gelatin film. They also concluded that the transparency of the film deteriorated with a higher loading of tannic acid (which corroborates that a slight phase separation took place). As discussed, the transparency of our film was also reduced with higher loading of tannic acid in Set II (B) and Set IV (D, E and F).

Water uptake and solubility studies

The effect of NCC loading and tannic acid on the water solubility and moisture content in chitosan is illustrated in Fig. 8. Since the focus of this analysis is on the suitability of this material for a wing membrane of a BMAV, water resistivity is one of the key performance factors. Set I has a water uptake equal to 224 % of its original dry mass (Fig. 8a). The addition of NCC drastically reduces the swelling and solubility of neat chitosan film (Fig. 8a, b). NCC increases the concentration of nanocrystal networks in the chitosan matrix, which are not involved in binding water molecules. NCC also increases the hydrogen bonding between the amino and sulphate ester groups, leaving no room for the OH group to interact with water molecules. A similar trend was observed in past research by Pereda et al. (2014), where the addition of cellulose nanocrystal in polyelectrolyte based chitosan/olive oil film reduces the total solubility matter and moisture sorption of the film. The addition of

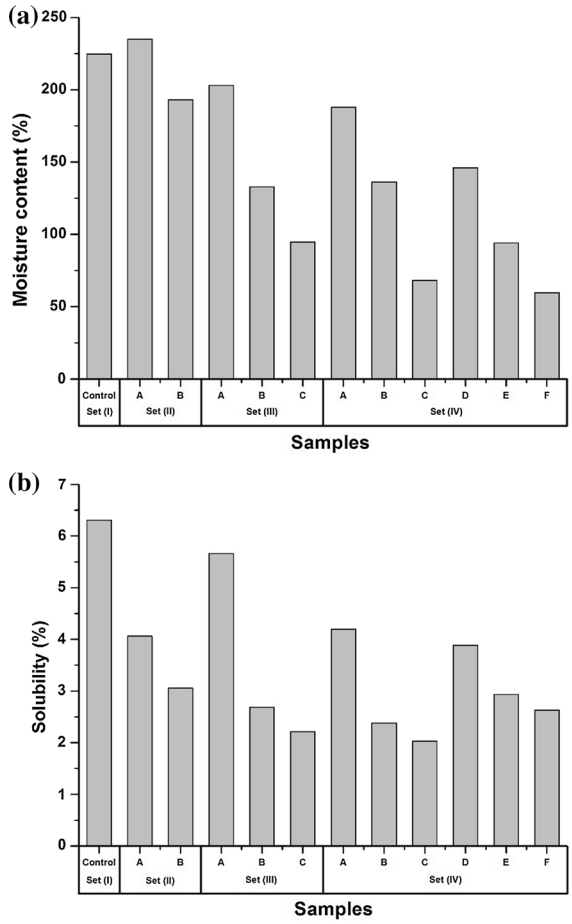

Fig. 8 Physicochemical characterization of all sample sets under equilibrium condition at 25 °C and 65 % relative humidity, **a** moisture content, **b** solubility of samples

tannic acid on the neat chitosan film and nanocomposite films (Sets II and IV) also decreased the water uptake and solubility. According to Rivero et al. (2010), who studied the heat treatment effects on chitosan based film, observed that (at high temperatures) chitosan film crosslinked with tannic acid showed a reduction in moisture uptake. They postulated that this was due to carboxylic acids reacting with the amine group to form an amide, thus eliminating water. Since this test was conducted after exposing the samples to a temperature of 105 °C for 1.5 h, the effectiveness of the crosslink increases the hydrophobic and/or hydrogen interaction between chitosan and tannic acid. Therefore this experiment shows that the water solubility and uptake on chitosan film can be controlled by adding tannic acid and NCC.

Comparison with film using chitin whiskers as a filler material

In previous work, chitin whiskers were used as filler material. The tensile and water uptake is compared with this experiment. These two parameters are important in determining the performance of the film. Figure 9a shows the tensile strength of selected sample sets with identical filler and tannic acid loading. With 10 % of filler content, NCC shows a higher increment in tensile strength when compare to chitin whiskers. Increasing tannic acid to 40 mg/chitosan into this filler loading yields the highest tensile strength of 61.5 MPa for NCC film (Set IV D). However further loading of filler content (30 %) doesn't give any significant increment for NCC and there is a decrease in tensile strength in 40 mg/chitosan for film Set IV (E). This indicates that the percolation threshold for NCC is faster than chitin whiskers. Chitin whiskers do not have this trend. Incrementally increasing the filler loading (up to 30 %), results in a steady increase of the tensile strength (without any adverse effects).

Figure 9b compares the water uptake. This figure shows the moisture content for selected samples of NCC and chitin whiskers. Compared to chitin whiskers, the NCC exhibited better resistance to water uptake with increased loading of filler material, regardless of tannic acid addition. Since both chitin and cellulose are hydrophobic in nature, the effectiveness of NCC in the chitosan matrix is better than chitin whiskers for water uptake capability.

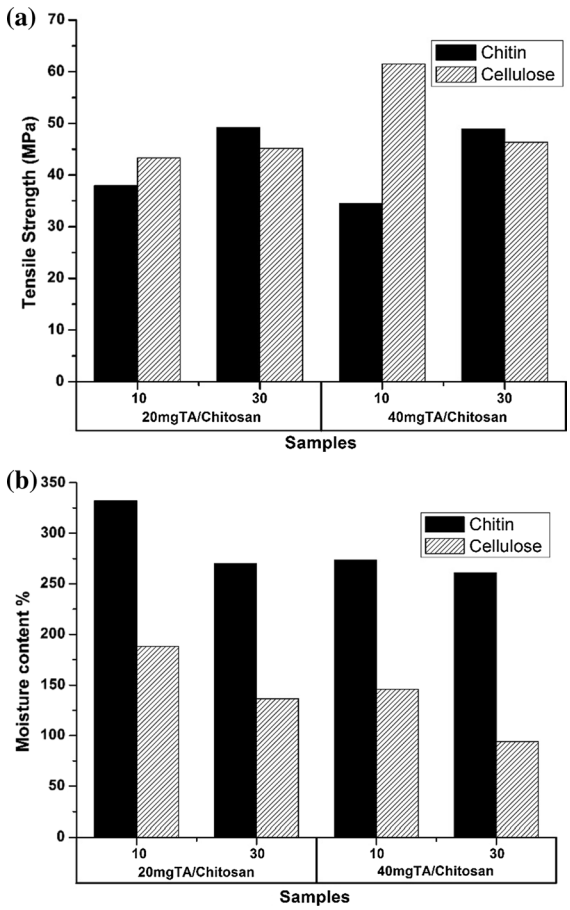

Fig. 9 Comparison of chitosan film with different filler material **a** tensile strength, **b** moisture content

Conclusion

It was observed that NCC as a filler material and tannic acid as a crosslinker improves the mechanical and physicochemical properties of chitosan film. TEM images confirm that the NCC particles are nanometer-scaled and possess a high aspect ratio. The XRD pattern shows that addition of NCC induces a combination of amorphous and crystalline regions in the chitosan matrix, which elevates the mechanical properties due to the formation of a percolating network and strong filler matrix interaction. The addition of NCC also reduces the water solubility and water uptake. Crosslinking the nanocomposite film with tannic acid also improves the mechanical and physicochemical properties (until it reaches a percolation limit). The XRD pattern shows that the addition of tannic acid changes the film into an anhydrous crystalline conformation. These film properties are well suited for use in BMAV wing membranes and other lightweight applications (e.g. packaging materials).

Acknowledgments This research was done under the auspices of the Centre for Transportation Research at the Faculty of Engineering, University of Malaya. It is primarily funded by High Impact Research Grant UM.C/625/1/HIR/MOHE/ENG/53 (H-16001-D000053) along with several other secondary Grants: RG155-12AET, RP011A-13AET, FP030-2013A, RU022B-2014, and RU022A-2014.

References

Aelenei N, Popa M, Novac O, Lisa G, Balaita L (2009) Tannic acid incorporation in chitosan-based microparticles and

in vitro controlled release. J Mater Sci Mater Med 20:1095–1102. doi:10.1007/s10856-008-3675-z

Azizi Samir MAS, Alloin F, Dufresne A (2005) Review of recent research into cellulosic whiskers, their properties and their application in nanocomposite field. Biomacromolecules 6:612–626. doi:10.1021/bm0493685

Badawy MI, Rabea E (2014) Synthesis and antifungal property of *N*-(aryl) and quaternary *N*-(aryl) chitosan derivatives against Botrytis cinerea. Cellulose 21:3121–3137. doi:10.1007/s10570-014-0333-0

Bigi A, Cojazzi G, Panzavolta S, Rubini K, Roveri N (2001) Mechanical and thermal properties of gelatin films at different degrees of glutaraldehyde crosslinking. Biomaterials 22:763–768. doi:10.1016/S0142-9612(00)002362

Bondeson D, Mathew A, Oksman K (2006) Optimization of the isolation of nanocrystals from microcrystalline cellulose by acid hydrolysis. Cellulose 13:171–180. doi:10.1007/s10570-006-9061-4

Brugnerotto J, Lizardi J, Goycoolea FM, Argüelles-Monal W, Desbrières J, Rinaudo M (2001) An infrared investigation in relation with chitin and chitosan characterization. Polymer 42:3569–3580. doi:10.1016/S0032-3861(00)00713-8

Cao N, Fu Y, He J (2007) Mechanical properties of gelatin films cross-linked, respectively, by ferulic acid and tannin acid. Food Hydrocoll 21:575–584. doi:10.1016/j.foodhyd.2006.07.001

Cranston ED, Gray DG (2006) Morphological and optical characterization of polyelectrolyte multilayers incorporating NCC. Biomacromolecules 7:2522–2530. doi:10.1021/bm0602886

de Mesquita JP, Donnici CL, Pereira FV (2010) Biobased nanocomposites from layer-by-layer assembly of cellulose nanowhiskers with chitosan. Biomacromolecules 11:473–480. doi:10.1021/bm9011985

de Souza Lima MM, Borsali R (2004) Rodlike Cellulose Microcrystals: structure, properties, and applications. Macromol Rapid Commun 25:771–787. doi:10.1002/marc.200300268

Goede M, Stehlin M, Rafflenbeul L, Kopp G, Beeh E (2009) Super Light Car lightweight construction thanks to a multi-material design and function integration. Eur Transp Res Rev 1:5–10. doi:10.1007/s12544-008-0001-2

Gopalan Nair K, Dufresne A (2003) Crab shell chitin whisker reinforced natural rubber nanocomposites. 2. Mechanical behavior. Biomacromolecules 4:666–674. doi:10.1021/bm0201284

Henson GL, Niemeyer L, Ansong G, Forkner R, Makkar HPS, Hagerman AE (2004) A modified method for determining protein binding capacity of plant polyphenolics using radiolabelled protein. Phytochem Anal 15:159–163. doi:10.1002/pca.762

Kabiri R, Namazi H (2014) NCC acetate (NCCA)/graphene oxide (GO) nanocomposites with enhanced mechanical properties and barrier against water vapor. Cellulose 21:3527–3539. doi:10.1007/s10570-014-0366-4

Khan A et al (2012) Mechanical and barrier properties of NCC reinforced chitosan based nanocomposite films. Carbohydr Polym 90:1601–1608. doi:10.1016/j.carbpol.2012.07.037

Kroustalli A et al (2013) Carbon nanotubes reinforced chitosan films: mechanical properties and cell response of a novel biomaterial for cardiovascular tissue engineering. J Mater Sci Mater Med 24:2889–2896. doi:10.1007/s10856-013-5029-8

Kushleyev A, Mellinger D, Powers C, Kumar V (2013) Towards a swarm of agile micro quadrotors. Auton Robots 35:287–300. doi:10.1007/s10514-013-9349-9

Leceta I, Guerrero P, de la Caba K (2013) Functional properties of chitosan-based films. Carbohydr Polym 93:339–346. doi:10.1016/j.carbpol.2012.04.031

Leung AW, Lam E, Chong J, Hrapovic S, Luong JT (2013) Reinforced plastics and aerogels by NCC. J Nanopart Res 15:1–24. doi:10.1007/s11051-013-1636-z

Li Q, Zhou J, Zhang L (2009) Structure and properties of the nanocomposite films of chitosan reinforced with cellulose whiskers. J Polym Sci Part B Polym Phys 47:1069–1077. doi:10.1002/polb.21711

Lu Y, Weng L, Zhang L (2004) Morphology and properties of soy protein isolate thermoplastics reinforced with chitin whiskers. Biomacromolecules 5:1046–1051. doi:10.1021/bm034516x

Ma H, Zhou B, Li H-S, Li Y-Q, Ou S-Y (2011) Green composite films composed of NCC and a cellulose matrix regenerated from functionalized ionic liquid solution. Carbohydr Polym 84:383–389. doi:10.1016/j.carbpol.2010.11.050

Ma B, Qin A, Li X, Zhao X, He C (2014) Structure and properties of chitin whisker reinforced chitosan membranes. Int J Biol Macromol 64:341–346. doi:10.1016/j.ijbiomac.2013.12.01

Miao C, Hamad W (2013) Cellulose reinforced polymer composites and nanocomposites: a critical review. Cellulose 20:2221–2262. doi:10.1007/s10570-013-0007-3

Moon RJ, Martini A, Nairn J, Simonsen J, Youngblood J (2011) Cellulose nanomaterials review: structure, properties and nanocomposites. Chem Soc Rev 40:3941–3994. doi:10.1039/C0CS00108B

Nikonenko NA, Buslov DK, Sushko NI, Zhbankov RG (2005) Spectroscopic manifestation of stretching vibrations of glycosidic linkage in polysaccharides. J Mol Struct 752:20–24. doi:10.1016/j.molstruc.2005.05.015

Orlowski CT, Girard AR (2012) Dynamics, stability, and control analyses of flapping wing micro-air vehicles. Prog Aerosp Sci 51:18–30. doi:10.1016/j.paerosci.2012.01.001

Parker G (2010) Biomimetically-inspired photonic nanomaterials. J Mater Sci Mater Electron 21:965–979. doi:10.1007/s10854-010-0164-1

Peña C, de la Caba K, Eceiza A, Ruseckaite R, Mondragon I (2010) Enhancing water repellence and mechanical properties of gelatin films by tannin addition. Bioresour Technol 101:6836–6842. doi:10.1016/j.biortech.2010.03.112

Peng BL, Dhar N, Liu HL, Tam KC (2011) Chemistry and applications of NCC and its derivatives: a nanotechnology perspective. Can J Chem Eng 89:1191–1206. doi:10.1002/cjce.20554

Pereda M, Dufresne A, Aranguren MI, Marcovich NE (2014) Polyelectrolyte films based on chitosan/olive oil and reinforced with cellulose nanocrystals. Carbohydr Polym 101:1018–1026. doi:10.1016/j.carbpol.2013.10.046

Ritthidej GC, Phaechamud T, Koizumi T (2002) Moist heat treatment on physicochemical change of chitosan salt films. Int J Pharm 232:11–22. doi:10.1016/S0378-5173(01)00894-8

Rivero S, García MA, Pinotti A (2010) Crosslinking capacity of tannic acid in plasticized chitosan films. Carbohydr Polym 82:270–276. doi:10.1016/j.carbpol.2010.04.048

Rivero S, García MA, Pinotti A (2011) Heat treatment to modify the structural and physical properties of chitosan-based films. J Agric Food Chem 60:492–499. doi:10.1021/jf204077k

Rubentheren V, Ward TA, Chee CY, Tang CK (2015) Processing and analysis of chitosan nanocomposites reinforced with chitin whiskers and tannic acid as a crosslinker. Carbohydr Polym 115:379–387. doi:10.1016/j.carbpol.2014.09.007

Sabato SF, Ouattara B, Yu H, D'Aprano G, Le Tien C, Mateescu MA, Lacroix M (2001) Mechanical and barrier properties of cross-linked soy and whey protein based films. J Agric Food Chem 49:1397–1403. doi:10.1021/jf0005925

Syed HI, Richard VG, Baqar RZ (1999) Biopolymers vol 723. ACS Symposium Series, vol 723. American Chemical Society. doi:10.1021/bk-1999-0723

Takegawa A, Murakami M-A, Kaneko Y, Kadokawa J-I (2010) Preparation of chitin/cellulose composite gels and films with ionic liquids. Carbohydr Polym 79:85–90. doi:10.1016/j.carbpol.2009.07.030

Wang S-F, Shen L, Zhang W-D, Tong Y-J (2005) Preparation and mechanical properties of chitosan/carbon nanotubes composites. Biomacromolecules 6:3067–3072. doi:10.1021/bm050378v

Zhao J et al (2014) Reinforcement of all-cellulose nanocomposite films using native cellulose nanofibrils. Carbohydr Polym 104:143–150. doi:10.1016/j.carbpol.2014.01.007

Zhong L, Fu S, Peng X, Zhan H, Sun R (2012) Colloidal stability of negatively charged cellulose nanocrystalline in aqueous systems. Carbohydr Polym 90:644–649. doi:10.1016/j.carbpol.2012.05.091

Zuo P-P, Feng H-F, Xu Z-Z, Zhang L-F, Zhang Y-L, Xia W, Zhang W-Q (2013) Fabrication of biocompatible and mechanically reinforced graphene oxide-chitosan nanocomposite films. Chem Cent J 7:39